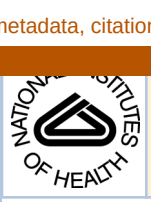

Published in final edited form as:

Toxicol Lett. 2013 October 24; 222(2): . doi:10.1016/j.toxlet.2013.07.014.

Methylmercury exposure increases lipocalin related (*lpr*) and decreases activated in blocked unfolded protein response (*abu*) genes and specific miRNAs in *Caenorhabditis elegans*

Martina Rudgalvyte[1], **Natalia VanDuyn**[2], **Vuokko Aarnio**[1], **Liisa Heikkinen**[1], **Juhani Peltonen**[1], **Merja Lakso**[1], **Richard Nass**[2], and **Garry Wong**[1,*]

[1]A. I. Virtanen Institute for Molecular Sciences, Department of Neurobiology, University of Eastern Finland, Kuopio, Finland [2]Department of Pharmacology and Toxicology, Indiana University School of Medicine, 635 Barnhill Drive, MS 549, Indianapolis, IN 46202, U.S.A.

Abstract

Methylmercury (MeHg) is a persistent environmental and dietary contaminant that causes serious adverse developmental and physiologic effects at multiple cellular levels. In order to understand more fully the consequences of MeHg exposure at the molecular level, we profiled gene and miRNA transcripts from the model organism *Caenorhabditis elegans*. Animals were exposed to MeHg (10μM) from embryo to larval 4 (L4) stage and RNAs were isolated. RNA-seq analysis on the Illumina platform revealed 541 genes up- and 261 genes down-regulated at a cutoff of 2-fold change and false discovery rate-corrected significance $q < 0.05$. Among the up-regulated genes were those previously shown to increase under oxidative stress conditions including *hsp-16.11* (2.5-fold), *gst-35* (10.1-fold), and *fmo-2*(58.5-fold). In addition, we observed up-regulation of 6 out of 7 lipocalin related (*lpr*) family genes and down regulation of 7 out of 15 activated in blocked unfolded protein response (*abu*) genes. Gene Ontology enrichment analysis highlighted the effect of genes related to development and organism growth. miRNA-seq analysis revealed 6–8 fold down regulation of *mir-37-3p*, *mir-41-5p*, *mir-70-3p*, and *mir-75-3p*. Our results demonstrate the effects of MeHg on specific transcripts encoding proteins in oxidative stress responses and in ER stress pathways. Pending confirmation of these transcript changes at protein levels, their association and dissocation characteristics with interaction partners, and integration of these signals, these findings indicate broad and dynamic mechanisms by which MeHg exerts its harmful effects.

Keywords

heavy metal; oxidative stress; ER stress; next-generation sequencing; blocked unfolded protein response

*To whom correspondence should be addressed: Professor Garry Wong, Ph.D., A.I. Virtanen Institute, University of Eastern Finland, PL1627, Kuopio 70211 FINLAND, ph:+358-44-2121319 fax:+358-17-163030.

Conflict of Interest Statement

The authors declare that they have no conflicts of interest.

1. Introduction

Methylmercury (MeHg) is a global contaminant that originates from inorganic mercury and accumulates in the environment. It has been found in a broad range of living organisms including plants, wildlife, and humans (WHO, 1990) who are exposed to mercury mostly through ingestion of contaminated seafood and fish, but can also be exposed through occupational hazards and via dental procedures (European Food Safety Authority, 2004; Björkman et a., 2007). After exposure, high concentrations of mercury are found in the brain as well as in blood, kidneys, and hair (Clarkson and Magos, 2006). MeHg easily crosses the blood-brain, blood-placenta and blood-retinoic barriers. It is associated with human developmental abnormalities, neurological dysfunction, embryonic defects, and loss of vision (Takeuchi, 1968). While the developing fetus is highly sensitive, in adult humans, MeHg poisoning can cause loss of physical coordination, abnormal speech, neuropathology, and death (Harada, 1968; Harada, 1978; Eto, 1997). Despite over 50 years of experience with human disasters, MeHg exposure remains a serious human health threat and its consequences continue to be intensely studied (Dórea et al., 2012; Aslan et al., 2013).

While the physical effects of MeHg toxicity are well documented, the molecular targets remain obscure. MeHg depletes glutathione, confers an increase in reactive oxygen species (ROS), mitochondrial dysfunction, oxidative phosphorylation, and a loss of calcium regulation (Clarkson and Magos, 2006; Choi et al., 1996). Strategies to attenuate the toxic effects of MeHg include administering antioxidants, chelators, or increasing metallothioneins to promote removal (Choi et al., 1996; Miles et al., 2000; Boscola et al., 2010). Due to MeHg's role in oxidative stress, it has been hypothesized that mitochondria are an intracellular target, but associations with endoplasmic reticulum (ER), Golgi complex, nuclear envelope, and lysosomes have also been observed (Chang et al., 1977; Limke et al., 2004; Ceccatelli et al., 2010; Roos et al., 2012). Mercury ions form cross-linkages with membrane proteins causing structural disorganization and weakening of the architecture of membranes that leads to neurotoxic events (Baatrup 1991; Barboni el al. 2008). MeHg mimics the amino acid methionine by forming MeHg-L-cysteine complexes. It has been suggested that the Hg reaction with proteins is non-specific: Hg ions react with any sulfhydryl group forming S-HG-S bridges (Miura and Imura, 1987). MeHg diffuses across cell membranes as well as other cell compartments and interfere not only with cell membrane proteins, but also with internal cell proteins. These events disturb crucial cell processes and decrease cell integrity, disrupt migration and change cell signaling that ultimately leads to altered cell function (Limke et al., 2004; Ceccatelli et al., 2010; Roos et al., 2012).

Previous genome level studies aimed at elucidating the downstream transcriptional effects of MeHg have found the targets of the oxidative stress-activated transcription factor Nrf2 to be upregulated including cell cycle, apoptosis, cytokine, and heat shock genes as well as adaptive response genes that include chemokines, glutathione S-transferases, metallothioneins, and thioredoxin peroxidases (Liu et al., 2003; Simmons et al., 2011; Ayensu and Tchounwou 2006). While these previous studies have been highly informative, they mainly focused on specific target tissues. For example, the studies profiled rat liver and kidneys (Hendriksen et al., 2007), rat lungs (Liu et al., 2003) mice pup brains (Glover et al., 2009), metallothionein-I/II null mice brains (Yoshida et al., 2011), or zebrafish liver (Ung et al., 2010). Other studies used cell lines such as HepG2 (Kawata et al., 2007; Avensu and Tchounwou, 2006). Simmons and colleagues (2011) demonstrated a variability between cell lines in activity and relative potency in response to MeHg and other heavy metals.

The nematode *Caenorhabditis elegans* is a convenient tool for toxicological studies (Nass and Hamza, 2007). Since molecular mechanisms in development, cell migration and toxicity

are analogous on many levels in *C. elegans* and humans, and they also share similarities in signaling and neurotransmitter systems, this animal has been a useful tool in basic human pathophysiology studies. We previously demonstrated that chronic exposure to MeHg reduces the brood size and number of viable eggs, and affects viability and development of the embryo with delays in morphogenesis and gonadogenesis, and dopamine neuron degeneration (VanDuyn et al., 2010). We also demonstrated the transcriptional regulation of a variety of oxidative sress response genes, including glutathione S-transferases that were dependent upon the transcription factor SKN-1, the *C. elegans* ortholog of Nrf2 (VanDuyn et al., 2010).

In the current study, we investigated the effect of MeHg on global gene transcription in whole animals. This approach was used to cover, as broadly as possible, tissue or cell specific responses. Moreover, we exposed animals from embryo to larval 4 (L4) stage, a stage just prior to adulthood, modeling a chronic exposure, in order to uncover more chronic effects of heavy metal exposure. In addition, we used highly sensitive RNA-seq methodology coupled with Gene Ontology enrichment analysis, to identify both individual genes and overrepresented Gene Ontology terms. Finally, we used miRNA-seq as a global approach to identify miRNAs whose expression was altered following MeHg exposure in whole animals.

2. Materials and Methods

2.1. *C. elegans* maintenance and treatment

C. elegans strains wild-type (WT) Bristol N2, RNAi-sensitive mutant NL2099 (*rrf-3(pk1426)*), and transgenic JS4063 (P*abu-1*::GFP) were obtained from the Caenorhabditis Genetics Center (St. Paul, MN, U.S.A.) and maintained on nematode growth media (NGM) plates with bacterial lawns containing OP50 strain *E. coli* bacteria at 20°C according to standard procedures (Brenner, 1974). Synchronized worms were obtained by bleaching gravid adults in potassium hypochlorite and washed 4 X in M9 buffer. Embryos were placed directly onto NGM plates seeded with OP50. Methylmercury(II)Cl (MeHg) (Sigma, St. Louis, MO, U.S.A.) was dissolved in distilled water and kept as a 500 μM stock solution and then added to agar plates for a final concentration of 10μM. Control plates were without MeHg added. Animals were allowed to grow at 20 °C until reaching L4 stage just before adulthood (48–56 h) for RNA isolation.

2.2. RNA isolation and sequencing

For RNA isolation both control and MeHg-treated L4 stage worms were collected, washed 4X with sterile water and placed immediately into Trizol solution (Gibco-BRL, Gaithersberg, MD, USA). Total RNA was isolated according to manufacturer's protocol and quantitated on a Nanodrop device (Thermo Scientific, Wilmington, DE, USA). Total RNAs were then treated to remove DNA using Turbo DNA-free DNAse kit (Ambion, Austin, TX, USA). Isolated and DNAse treated total RNA was then sequenced using Illumina library sample kit (Illumina, San Diego, CA, USA) on a GA IIx instrument, using single read 38 nt mode.

2.3. RNA-seq analysis

35.4 million and 41.1 million sequences of 38 bases were acquired from the control and MeHg-treated samples, respectively. Reads containing adapters (536533 and 615796 for control and MeHg-treated samples, respectively) were removed with TagDust 1.13 (Lassmann et al. 2009) using the default parameter values (28.0 % coverage cutoff and 0.01 FDR). To find reads arising from the food source *E. coli*, the remaining reads were aligned to *E. coli* genome (version st 536, NCBI) with Bowtie 0.12.7 (Langmead et al. 2009)

allowing 0 mismatches. Reads aligning to the *E. coli* genome (1562 and 20449, respectively) were removed from further steps of the analysis. The remaining reads were then aligned to *C. elegans* genome (WormBase WS220, Ensembl Release 66) and known splice junctions derived from the gene annotation file ws220/genes.gtf with TopHat 2.0.3 (Trapnell et al. 2009) using the following parameter values: --no-novel-juncs, --min-intron-length 10, --max-intron-length 25000, --min-segment-intron 10, --max-segment-intron 25000, --min-coverage-intron 10, --max-coverage-intron 1000, --max-multihits 10, --transcriptomemismatches 1, --genome-read-mismatches 1, --read-mismatches 1, --segment-mismatches 1, -- bowtie-n, -G /ws220/genes.gtf.

Differential gene expression analysis was performed using Cuffdiff program of Cufflinks 1.3.0 (Trapnell et al. 2010) for 44968 predicted transcripts. Transcripts with false discovery rate-corrected *p*-values (*q*-values) of < 0.05 and fold change > 2 (or <0.5) were defined as differentially expressed. Enriched Gene Ontology terms (The Gene Ontology Consortium, 2000) were found separately for the up-regulated and down-regulated genes from DAVID Functional Annotation Tool (Huang et al., 2009).

2.4. miRNA-seq analysis

Small RNAs (<200bp) were isolated from L4 animals after treatment with MeHg (10 μM) since embryo stage using the miRVana kit (Ambion) according to the manufacturer's instructions. One μg of isolated small RNAs were used to construct a library using the Small RNA library prep set kit for Illumina (New England Biolabs, Ipswich, MA, USA) using the same conditions as reported previously (Srinivasan et al., 2013). Library products were sequenced on Illumina GAIIx instrument in single read 38nt mode.

The sizes of the small RNA sequence libraries were 21.9 million reads for the control and 23.3 million reads for the MeHg treated sample. From the raw data reads, 3' adapters were trimmed and adapter dimers were removed using in-house tools. Further, reads exactly mapping to *E. coli* genome were removed from the libraries. Of the preprocessed data including 20.8 million reads in the control and 22.1 million reads in the treated sample, 85 % and 84 %, respectively, mapped to the *C. elegans* genome (WS220) with max one mismatch. Alignment to the genome was performed with Bowtie 0.12.9, (Langmead et al. 2009). Known miRNAs (miRBase Release 19) were identified and calculated with miRDeep 2.0.0.5 (Friedländer et al., 2012). Differential expression analysis was conducted for miRNAs with at least 1 RPM expression with DESeq 1.6.1 (Anders and Huber, 2010). miRNA targets were predicted with miR-SOM (Heikkinen et al., 2011) and targets of *lpr* and *abu* genes with TargetScan worm 6.2 (Jan et al. 2011).

2.5. Quantitative real-time PCR (qRT-PCR)

The expression of 13 genes was analyzed by qRT-PCR based on RNA-seq findings. Four independent biological replicate total RNA samples from control and MeHg-treated (final concentration 10μM) *C. elegans* were isolated from L4 stage worms as described above. Total RNA was reverse transcribed to cDNA using Revert-Aid kit (Thermo Fisher Scientific, Waltham, MASS, USA) according to the manufacturer's instructions. Oligonucleotide primers for PCR were designed and obtained from Oligomer OY (Helsinki, Finland). The amplification reaction was performed according to the manufacturer's protocol with SYBR green PCR Master mix (Thermo Fisher, USA) using iCycler 1.0 (Biorad, Hercules, CA, USA). Each of 4 biological replicates was performed in duplicate technical replicates. Gene expression differences were calculated using the delta-delta-Ct method (Livak et al. 2001). The *act-1* gene, a highly abundant housekeeping transcript was used as an internal control. This gene has been used previously as the internal control for

qRT-PCR experiments under a wide variety of conditions and from different tissues and organisms. Sequences for all primer sets used are listed in Supplementary Table 1.

2.6. RNA interference

RNA-mediated interference (RNAi) was accomplished on NGM plates containing 1mM isopropyl β-D-thiogalactoside (IPTG) and 100μg/ml ampicillin. Plates were seeded with HT115 (DE3), an RNase III-deficient *E. coli* strain carrying L4440 vector with the gene fragment (*skn-1*) (Source BioScience LifeSciences, Nottingham, UK) or empty vector (Addgene, Cambridge, MA). Bacteria cultures were grown for 10 h in liquid medium with 100μg/ml ampicillin and without IPTG. After 10 h IPTG (1mM) was added, cultures were grown 4 h more and transferred onto plates. L1 stage worms or embryos were transferred onto RNAi plates and incubated at 20°C for 48–56 h for RNA isolation. Control RNAi was performed with HT115 bacteria containing an empty L4440 vector. RNAi of skn-1 was confirmed by qRT-PCR of skn-1 transcripts. For ABU family RNAi studies, NL2099 animals were fed separately RNAi bacteria of *abu-1, 6, 7, 9, 10,* and *11* for 48 h and then exposed to MeHg (10μM, 20μM, or 50μM) for 2 days and then animals were scored for death. For developmental studies, NL2099 animals were grown on ABU family RNAi bacteria from L1 stage on 1μM MeHg and time to adulthood was measured.

2.7. Fluorescence microscopy

JS4063 animals from control and MeHg-treated (final concentration 125μM) groups were placed on an agar pad with a drop of Aldicarb (final concentration 2.5mM) and a drop of Fluoroshield (Sigma Chemicals). In order to avoid drying, animals were imaged immediately on an Olympus IX71 (Olympus, Tokyo, Japan) fluorescent microscope. Images were taken with DP Controller software (version 2.1.1.227, Olympus) at magnification 100X.

3. Results

3.1. RNA-seq and miRNA-seq analysis of *C. elegans* exposed to MeHg

A total of 35.4 million and 41.1 million sequence reads were produced from sequencing RNA-seq libraries from control and MeHg-treated samples, respectively. From Cufflinks RNA-seq data analysis program, using criteria of > 2 fold change and false discovery rate (FDR) corrected *p*-value (*q*-value) < 0.05, 802 genes were found to be regulated, of which 541 were up and 267 were down (Figure 1A). The complete list of regulated genes are in Supplementary Table 2. Known oxidative stress responsive genes up-regulated included *hsp-16.11* (2.5-fold), *gst-35* (10-fold), and *fmo-2* (58-fold). The largest fold change was the downstream of *daf-16* gene *dod-21* which was up-regulated > 890-fold. The genes with the 20 largest fold-changes up and down and their FPKM (fragments per kilobase of exon per million fragments mapped) values are shown in Table 1.

From miRNA-seq analysis we were able to identify 4 mature miRNA sequences significantly altered after MeHg exposure (Figure 1B). All were down regulated in MeHg animals ($p < 0.05$): *miR-37-3p*, 7.5-fold; *miR-75-3p*, 7.8-fold; *miR-70-3p*, 5.7-fold; *miR-41-5p*, 6.5-fold. The complete list of miRNAs and expression values can be found in Supplementary Table 3. Using a miRNA target prediction software TargetScanWorm 6.2 (Jan et al. 2011) and miRSOM (Heikkinen et al., 2010) we looked for potential targets of miRNA from our list of regulated RNAs. We were not able to find *lpr* or *abu* family genes on the candidate target lists. We also looked at the possible miRNAs that would regulate *lpr* and *abu* gene families and these also did not overlap with the found regulated miRNAs.

3.2. qRT-PCR confirms LPR and ABU genes

A large number of LPR (LiPocalin-Related protein) and ABU (Activated in Blocked Unfolded protein response) family members were found to be regulated. The LPR genes included *lpr-1, lpr-3, lpr-4, lpr-5, lpr-6, lpr-7* from a total of 7 family members. The *abu* genes included *abu-1, abu-6, abu-7, abu-8, abu-9, abu-10,* and *abu-11* from a total of 15 family members. In order to verify the gene regulation, we performed qRT-PCR on the 13 genes from ABU and LPR gene families using four independent MeHg-treated and control samples from L4 animals (Figure 2). The 6 LPR family members were confirmed to be up-regulated and all 7 ABU family members were confirmed to be down-regulated significantly. The most highly decreased *abu* gene based on qRT-PCR results was *abu-1* (20-fold down), while RNA-seq showed a lower but still robust 7-fold change down. Other ABU family genes were also confirmed to be down-regulated. The *lpr* genes had more modest fold changes in qRT-PCR than in RNA-seq. The most highly up-regulated *lpr* gene, *lpr-4*, according to RNA-seq (31-fold) was only 2-fold up-regulated in qRT-PCR. Other LPR family genes also share similar fold change differences comparing RNA-seq and qRT-PCR results but are consistently up-regulated according to both methods.

3.3. *abu-1* transcriptional regulation to MeHg is not dependent upon *skn-1* expression

MeHg (10 μM) exposure from embryo to L4 decreased *abu-1* expression in *skn-1* RNAi animals (0.67 ± 0.20, n=4) relative to non-exposed animals, and also in HT115 no-RNAi control animals (0.52 ± 0.17, n=4). No significant difference was detected between *abu-1* expression after MeHg exposure in *skn-1* and control RNAi treatments (p=0.31). *skn-1* RNAi treatments decreased *skn-1* expression 3.0 ± 0.77 fold. MeHg increased *lpr-1* expression in *skn-1* RNAi animals (2.1 ± 0.34, n=4) while the increases were 1.1 ± 0.34, n=4 in HT115 RNAi animals. We also performed RNAi of *abu-1, 6, 7, 9, 10*, and *11* and measured sensitivity to MeHg at 10μM, 20μM, or 50μM, for 48 h. We were not able to find any differences in sensitivity as measured by percentage of live animals at any of the concentrations tested, or time to reach adulthood on 1μM MeHg (data not shown).

3.4. Functional annotation and GO enrichment analysis of regulated genes

In order to uncover biological themes of genes regulated by MeHg, we utilized the DAVID functional annotation tool to annotate, extract, and then analyze for statistical enrichment of Gene Ontology (GO) biological processes, cell compartments or molecular functions (Table 2). Enriched biological processes for up regulated genes were related to e.g. cuticle development (15 genes), organism growth (25 genes), protein maturation and processing (7 genes), and larval development (54 genes). A large number of up-regulated genes (190) belong to cellular compartment integral and/or intrinsic to membrane. One of the genes from this list is lipocalin-related protein gene *lpr-1*. The most represented up-regulated genes in the endoplasmic reticulum (Table 2) belong to FK506-binding protein family (*fkb-3, fkb-4, fkb-5, fkb-7*) or Flavin-containing MonoOxygenase family (*fmo-2, fmo-4*) (data not shown). The most represented down-regulated genes in cytoskeleton and intracellular non-membrane-bounded organelle are major sperm protein genes (5 genes, data not shown).

3.5. P*abu-1*::GFP strain shows response to MeHg

To confirm reduced *abu-1* gene expression , transgenic integrated P*abu-1::GFP* strain JS4063 was used. Transgenic animals express GFP strongly in the pharynx. Fluorescence intensity in young adults was measured 24 h after exposure to MeHg (125μM) for 1 h. A higher dose was used for GFP studies since lower doses did not produce observable effects (data not shown). Reduced fluorecence intensity in C. elegans pharynx, especially in the procorpus region was observed in ~30% of the animals (Figure 3). Three independent experiments were performed for this study.

4. Discussion

Previous studies have demonstrated that exposure to MeHg causes an oxidative stress response in cells, as well as increases in reactive oxygen species (ROS), disruption of respiration, oxidative phosphorylation and calcium regulation (Yee and Choi, 1996; Limke et al., 2004; Ceccatelli et al., 2010; Roos et al., 2012). Cellular responses to MeHg include not only increases in glutathione content and glutathione-S-transferases (GSTs), but also other protein groups such as HSPs and MTs. The present study detected many genes that confirm this notion. We also observed genes that suggest an ER response. ABU proteins form part of the ER stress pathway that responds to unfolded proteins and are distantly related to the apoptosis pathway gene CED-1 (Hetz, 2012). Many ABU gene family members were down-regulated in this study. ABU transcripts have been found to be activated when the unfolded protein response (UPR), a central process of ER stress, is blocked either genetically or pharmacologically (Shen et al., 2001; Yoshida et al., 2001; Urano et al., 2002). Previous studies have found SIR-2.1 (not regulated in this study, Supplementary Table 2) and OCTR-1 (not regulated in this study, Supplementary Table 2) to repress *abu-11* or ABU family member expression, respectively (Viswanathan et al., 2005; Sun et al., 2011). We did not see an influence by SKN-1 on *abu-1* response to MeHg in RNAi experiments. Therefore, the transcription factor(s) controlling *abu* gene expression remains to be identified. The decrease in *abu-11* expression in *C. elegans* following gold nanoparticle exposure (Tsyusko et al., 2012) or in *abu* gene family members after chronic ethanol exposure (Peltonen et al., 2013); however, suggest a common general xenobiotic responsive transcription factor.

The UPR functions to ensure that protein synthesis, folding and degradation rate match cell needs in order to avoid over accumulation of proteins in ER. It has been hypothesized that incorrect protein accumulation in the ER and UPR alterations may lead to the emergence of human diseases such as atherosclerosis or neurodegeneration (Malhotra and Kaufman, 2007). Studies have shown that oxidative stress, hypoxic stress, or nutrient stress can activate the UPR pathway (Wang and Kaufman, 2012). A classic marker for ER stress activation in mammlian cells is CHOP and this would have been useful to test, however no *C. elegans* orthologs exists to our knowledge (Marciniak et al., 2004). We also observed the regulation of oxidative stress markers such as *fmo, hsp,* and *gst* genes. However, separating the oxidative stress response from the ER stress responses may be difficult. For example, two flavin mono-oxygenease genes, *fmo-2* and *fmo-4*, were grouped into the endoplasmic reticulum (ER) class of proteins by gene enrichment analysis, but these genes could also be considered markers of oxidative stress. Also found within this class were four FK506 binding proteins. These proteins were originally classed as peptidyl prolyl cis-trans isomerases (PPIase) involved in protein folding. However, they were later found to be histone chaperones involved in the regulation of rDNA silencing, and suggests a potential novel mechansim by which MeHg could regulate developmental processes (Kuzuhara and Horikoshi, 2004).

The *lpr* gene family is known to play an important role in excretory duct cell development. The *lpr-1* gene is required for luminal connectivity between excretory duct and pore cell in excretory system of *C. elegans* (Stone el al. 2009). In the present study, we showed up-regulation of multiple LPR family members. Lipocalin sequences are diverse, however, they share functional and structural conservation. Most lipocalins have 1–3 disulfide bonds and an eight strand anti-parallel, symmetrical beta barrel fold, however, it is the function of a human lipocalin (Von Ebner's Gland of the tongue (VEGh), that acts as a cysteine protease inhibitor that suggests increases in lipocalin may be a response to increase protection of cysteine containing proteins (van't Hof et al., 1997). Increases in GSTs could also be elicited by methylmercury for 2 reasons: first, as a general response due to oxidative stress

(vanDyun et al., 2010), and secondly, perhaps to directly facilitate the removal of methylmercury via glutathione S-transferase activity. Coupled with the historical literature demonstrating mercury as an effective nephrotoxin (Edwards, 1942; Rodin and Crowson, 1962), and the current literature advocating lipocalin as an indicator of kidney damage (Mori and Nakao, 2007), our results would suggest a novel link between nematodes and humans in an aspect nephrotoxicity. The increases in LPR family gene expression after chronic MeHg exposure are consisent with cellular damage since acute exposure for 3h in MeHg (10μM) resulted in only very modest 0.9 –1.7 fold changes in LPR family members (data not shown). In addition, our RNA-seq and qRT-PCR data show quantitative but not qualitative differences. While the high sensitivity and dynamic range of RNA-seq for detecting and quantitating gene expression has been established, few studies have compared directly RNA-seq versus qRT-PCR. Lee et al, 2010 compared 27 randomly selected genes for such as comparison. While correlation was good (r^2 = 0.62–0.90), it depended upon the RNA-seq data processing method used, gene isoform, and level of expression. Clearly, RNA-seq methods still require improved and standardized methods to provide more accurate expression values. These improvements and their implementation will likely lead to better agreement between different gene expression level detection platforms.

We observed 4 miRNAs that were significantly altered in MeHg exposed animals, yet their predicted targets did not overlap our regulated genes list. Several possible scenarios could account for this: first, miRNA target prediction remains difficult with many false positives/negatives and few known validated hits; second, miRNAs could act locally and thus a whole animal approach such as was used here could dilute any miRNA or mRNA differences; finally, the whole animal approach limits the ability to know the anatomical source of the miRNA and its target, thus limiting the ability to detect miRNA-mRNA target combinations that might be regulated modestly but are closely linked anatomically. Novel single cell RNA-seq methods are now becoming feasible and may eventually be able to help to tease apart the precise interactions between miRNAs and mRNAs at the single cell level (Tang et al., 2010). Moreover, miRNAs can in some cases repress translation of target mRNAs without markedly reducing their levels (Valencia-Sanchez et al. 2006).

In summary, we have identified 2 gene families and 4 miRNAs regulated following exposure to MeHg in *C. elegans*. The gene transcripts regulated suggest an important role for oxidative stress, ER stress, and excretory duct cell development pathways in mediating the toxic actions of MeHg. The results presented are at the transcript level, and therefore preliminary pending confirmation at the protein level, characterization of the status of protein interaction partners, intracellular locations, and integration of ER stress signals. While a broad array of pathways are involved, our studies suggest that individual genes that contribute to such actions can be elucidated using a global transcriptomic approach.

Supplementary Material

Refer to Web version on PubMed Central for supplementary material.

Acknowledgments

The authors thank the Academy of Finland (M.L., G.W.), Biocenter Finland (L.H.), Finnish Cultural Foundation / Northern Savo Regional Fund (V.A.) and the doctoral program of molecular medicine at the University of Eastern Finland (M.R. and J.P.) for financial support. This study was partially supported by grants R011ES014459 and ES015559 from the National Institute of Environmental Health Sciences (RN) and an EPA STAR graduate fellowship (N.V.). We gratefully acknowledge Drs. Paul Sternberg and Igor Antoshechkin at the Millard and Muriel Jacobs Genetics and Genomics Laboratory, California Institute of Technology, for assistance with sequencing. We are indebted to Drs. Antero Salminen and Markus Storvik, and members of the NordForsk Nordic *C. elegans* Network for comments, suggestions, and encouragement. Some strains were provided by the

Caenorhabditis Genetics Center, which is funded by NIH Office of Research Infrastructure Programs (P40 OD010440).

References

Anders S, Huber W. Differential expression analysis for sequence count data. Genome Biol. 2010; 11:R106. [PubMed: 20979621]

Aslan L, Aslankurt M, Bozkurt S, Aksoy A, Ozdemir M, Gizir H, Yasar I. Ophthalmic findings in acute mercury poisoning in adults: A case series study. Toxicol Ind Health. 2013 Mar 22. 2013. [Epub ahead of print].

Ayensu WK, Tchounwou PB. Microarray analysis of mercury-induced changes in gene expression in human liver carcinoma (HepG2) cells: importance in immune responses. Int J Environ Res Public Health. 2006; 3:141–173. [PubMed: 16823088]

Baatrup E. Structural and functional effects of heavy metals on the nervous system, including sense organs, of fish. Comp Biochem Physiol. C. 1991; 100:253–257. [PubMed: 1677859]

Barboni MT, da Costa MF, Moura AL, Feitosa-Santana C, Gualtieri M, Lago M, Medrado-Faria Mde A, Silveira LC, Ventura DF. Visual field losses in workers exposed to mercury vapor. Environ Res. 2008; 107:124–131. [PubMed: 17719027]

Björkman L, Lundekvam BF, Laegreid T, Bertelsen BI, Morild I, Lilleng P, Lind B, Palm B, Vahter M. Mercury in human brain, blood, muscle and toenails in relation to exposure: an autopsy study. Environ Health. 2007; 6:30. [PubMed: 17931423]

Boscolo M, Antonucci S, Volpe AR, Carmignani M, Di Gioacchino M. Acute mercury intoxication and use of chelating agents. J Biol Regul Homeost Agents. 2009; 23:217–223. [PubMed: 20003760]

Brenner S. The Genetics of Caenorhabditis elegans. Genetics. 1974; 77:71–94. [PubMed: 4366476]

Ceccatelli S, Daré E, Moors M. Methylmercury-induced neurotoxicity and apoptosis. Chem Biol Interact. 2010; 188:301–308. [PubMed: 20399200]

Chang LW. Neurotoxic effects of mercury--a review. Environ Res. 1977; 14:329–373. [PubMed: 338298]

Choi BH, Yee S, Robles M. The effects of glutathione glycoside in methyl mercury poisoning. Toxicology and Applied Pharmacology. 1996; 141:357–364. [PubMed: 8975759]

Clarkson TW, Magos L. The toxicology of mercury and its chemical compounds. Crit Rev Toxicol. 2006; 36:609–662. [PubMed: 16973445]

Dórea JG, Marques RC, Isejima C. Neurodevelopment of Amazonian infants: antenatal and postnatal exposure to methyl- and ethylmercury. J Biomed Biotechnol. 2012; 2012:132876. [PubMed: 22619491]

Edwards JG. The renal tubule (nephron) as affected by mercury. Am. J. Path. 1942; 18:1011–1027. [PubMed: 19970664]

Eto K. Pathology of Minamata disease. Toxicol Pathol. 1997; 25:614–623. [PubMed: 9437807]

European Food Safety Authority. Opinion of the Scientific Panel on Contaminants in the Food Chain Related to Mercury and Methylmercury in Food. Brussels: European Food Safety Authority; 2004. EFSA-Q-2003-030.

Friedländer MR, Mackowiak SD, Li N, Chen W, Rajewsky N. miRDeep2 accurately identifies known and hundreds of novel microRNA genes in seven animal clades. Nucleic Acids Res. 2012; 40:37–52. [PubMed: 21911355]

Glover CN, Zheng D, Jayashankar S, Sales GD, Hogstrand C, Lundebye AK. Methylmercury speciation influences brain gene expression and behavior in gestationally-exposed mice pups. Toxicol Sci. 2009; 110:389–400. [PubMed: 19465457]

Harada, Y. Infantile Minamata disease. Japan: Kumamoto University; 1968. Minamata disease: Study group of Minamata disease; p. 73-92.

Harada Y. Congenital Minamata disease: Intrauterine methylmercury poisoning. Teratology. 1978; 18:285–288. [PubMed: 362594]

Heikkinen L, Kolehmainen M, Wong G. Prediction of microRNA targets in Caenorhabditis elegans using a self-organizing map. Bioinformatics. 2011; 27:1247–1254. [PubMed: 21422073]

Hendriksen PJ, Freidig AP, Jonker D, Thissen U, Bogaards JJ, Mumtaz MM, Groten JP, Stierum RH. Transcriptomics analysis of interactive effects of benzene, trichloroethylene and methyl mercury within binary and ternary mixtures on the liver and kidney following subchronic exposure in the rat. Toxicol Appl Pharmacol. 2007; 225:171–188. [PubMed: 17905399]

Hetz C. The unfolded protein response: controlling cell fate decisions under ER stress and beyond. Nat Rev Mol Cell Biol. 2012; 13:89–102. [PubMed: 22251901]

Huang DW, Sherman BT, Lempicki RA. Systematic and integrative analysis of large gene lists using DAVID Bioinformatics Resources. Nature Protoc. 2009; 4:44–57. [PubMed: 19131956]

Jan CH, Friedman RC, Ruby JG, Bartel DP. Formation, regulation and evolution of Caenorhabditis elegans 3'UTRs. Nature. 2011; 469:97–101. [PubMed: 21085120]

Kawata K, Yokoo H, Shimazaki R, Okabe S. Classification of heavy-metal toxicity by human DNA microarray analysis. Environ Sci Technol. 2007; 41:3769–3774. [PubMed: 17547211]

Kuzuhara T, Horikoshi M. A nuclear FK506-binding protein is a histone chaperone regulating rDNA silencing. Nat Struct Mol Biol. 2004; 11:275–283. [PubMed: 14981505]

Lassmann T, Hayashizaki Y, Daub CO. TagDust--a program to eliminate artifacts from next generation sequencing data. Bioinformatics. 2009; 25:2839–2840. [PubMed: 19737799]

Langmead B, Trapnell C, Pop M, Salzberg SL. Ultrafast and memory-efficient alignment of short DNA sequences to the human genome. Genome Biol. 2009; 10:R25. [PubMed: 19261174]

Lee S, Seo CH, Lim B, Yang JO, Oh J, Kim M, Lee S, Lee B, Kang C, Lee S. Accurate quantification of transcriptome from RNA-Seq data by effective length normalization. Nucleic Acids Res. 2011; 39:e9. [PubMed: 21059678]

Limke TL, Heidemann SR, Atchison WD. Disruption of intraneuronal divalent cation regulation by methylmercury: are specific targets involved in altered neuronal development and cytotoxicity in methylmercury poisoning? Neurotoxicology. 2004; 25:741–760. [PubMed: 15288506]

Liu J, Lei D, Waalkes MP, Beliles RP, Morgan DL. Genomic analysis of the rat lung following elemental mercury vapor exposure. Toxicol Sci. 2003; 74:174–181. [PubMed: 12730625]

Livak K, Schmittgen TD. Analysis of Relative Gene Expression Data Using Real-Time Quantitative PCR and the 2-ΔΔCt Method. Methods. 2001; 25:402–408. [PubMed: 11846609]

Marciniak SJ, Yun CY, Oyadomari S, Novoa I, Zhang Y, Jungreis R, Nagata K, Harding HP, Ron D. CHOP induces death by promoting protein synthesis and oxidation in the stressed endoplasmic reticulum. Genes Dev. 2004; 18:3066–3077. [PubMed: 15601821]

Malhotra JD, Kaufman RJ. The endoplasmic reticulum and the unfolded protein response. Semin Cell Dev Biol. 2007; 18:716–731. [PubMed: 18023214]

Malhotra JD, Kaufman RJ. ER stress and its functional link to mitochondria: role in cell survival and death. Cold Spring Harb Perspect Biol. 2011; 3:a004424. [PubMed: 21813400]

Miles AT, Hawksworth GM, Beattie JH, Rodilla V. Induction, regulation, degradation, and biological significance of mammalian metallothioneins. Crit Rev Biochem Mol Biol. 2000; 35:35–70. [PubMed: 10755665]

Miura K, Imura N. Mechanism of methylmercury cytotoxicity. Crit Rev Toxicol. 1987; 18:161–188. [PubMed: 3325226]

Mori K, Nakao K. Neutrophil gelatinase-associated lipocalin as the real-time indicator of active kidney damage. Kidney Int. 2007; 71:967–970. [PubMed: 17342180]

Nass R, Hamza I. The nematode C. elegans as an animal model to explore toxicology in vivo: solid and axenic growth culture conditions and compound exposure parameters. Chapter 1:Unit1.9. Curr Protoc Toxicol.

Peltonen J, Aarnio V, Heikkinen L, Lakso M, Wong G. Chronic ethanol exposure increases cytochrome P-450 and decreases activated in blocked unfolded protein response gene family transcripts in caenorhabditis elegans. J Biochem Mol Toxicol. 2013; 27:219–228. [PubMed: 23381935]

Rodin AE, Crowson CN. Mercury nephrotoxicity in the rat. 1. Factors influencing the localization of the tubular lesions. Am J Pathol. 1962; 41:297–313. [PubMed: 14493110]

Roos D, Seeger R, Puntel R, Barbosa NV. Role of Calcium and Mitochondria in MeHg-Mediated Cytotoxicity. J Biomed Biotechnol. 2012; 2012:248764. [PubMed: 22927718]

Simmons SO, Fan CY, Yeoman K, Wakefield J, Ramabhadran R. NRF2 Oxidative Stress Induced by Heavy Metals is Cell Type Dependent. Curr Chem Genomics. 2011; 5:1–12. [PubMed: 21643505]

Shen X, Ellis RE, Lee K, Liu CY, Yang K, Solomon A, Yoshida H, Morimoto R, Kurnit DM, Mori K, Kaufman RJ. Complementary signaling pathways regulate the unfolded protein response and are required for C. elegans development. Cell. 2001; 107:893–903. [PubMed: 11779465]

Srinivasan J, Dillman AR, Macchietto MG, Heikkinen L, Lakso M, Fracchia KM, Antoshechkin I, Mortazavi A, Wong G, Sternberg PW. The Draft Genome and Transcriptome of Panagrellus redivivus Are Shaped by the Harsh Demands of a Free-Living Lifestyle. Genetics. 2013; 193:1279–1295. [PubMed: 23410827]

Stone CE, Hall DH, Sundaram MV. Lipocalin signaling controls unicellular tube development in the Caenorhabditis elegans excretory system. Dev Biol. 2009; 329:201–211. [PubMed: 19269285]

Sun J, Singh V, Kajino-Sakamoto R, Aballay A. Neuronal GPCR controls innate immunity by regulating noncanonical unfolded protein response genes. Science. 2011; 332:729–732. [PubMed: 21474712]

Takeuchi, T. Pathology of Minamata disease. Japan: Kumamoto University; 1968. Minamata disease: Study group of Minamata disease; p. 141-228.

Tang F, Barbacioru C, Nordman E, Li B, Xu N, Bashkirov VI, Lao K, Surani MA. RNA-Seq analysis to capture the transcriptome landscape of a single cell. Nat Protoc. 2010; 5:516–535. [PubMed: 20203668]

Ashburner M, Ball CA, Blake JA, Botstein D, Butler H, Cherry JM, Davis AP, Dolinski K, Dwight SS, Eppig JT, Harris MA, Hill DP, Issel-Tarver L, Kasarskis A, Lewis S, Matese JC, Richardson JE, Ringwald M, Rubin GM, Sherlock G. The Gene Ontology Consortium. Gene ontology: tool for the unification of biology. Nat Genet. 2000; 25:25–29. [PubMed: 10802651]

Trapnell C, Pachter L, Salzberg SL. TopHat: Discovering splice junctions with RNA-seq. Bioinformatics. 2009; 25:1105–1111. [PubMed: 19289445]

Trapnell C, Williams BA, Pertea G, Mortazavi A, Kwan G, van Baren MJ, Salberg SL, Wold BJ, Pachter L. Transcript assembly and quantification by RNA-Seq reveals unannotated transcripts and isoform switching during cell differentiation. Nat Biotechnol. 2010; 28:511–515. [PubMed: 20436464]

Tsyusko OV, Unrine JM, Spurgeon D, Blalock E, Starnes D, Tseng M, Joice G, Bertsch PM. Toxicogenomic responses of the model organism Caenorhabditis elegans to gold nanoparticles. Environ Sci Technol. 2012; 46:4115–4124. [PubMed: 22372763]

Ung CY, Lam SH, Hlaing MM, Winata CL, Korzh S, Mathavan S, Gong Z. Mercury-induced hepatotoxicity in zebrafish: in vivo mechanistic insights from transcriptome analysis, phenotype anchoring and targeted gene expression validation. BMC Genomics. 2010; 11:212. [PubMed: 20353558]

Urano F, Calfon M, Yoneda T, Yun C, Kiraly M, Clark SG, Ron D. A survival pathway for Caenorhabditis elegans with a blocked unfolded protein response. J Cell Biol. 2002; 158:639–646. [PubMed: 12186849]

Vanduyn N, Settivari R, Wong G, Nass R. SKN-1/Nrf2 inhibits dopamine neuron degeneration in a Caenorhabditis elegans model of methylmercury toxicity. Toxicol Sci. 2010; 118:613–624. [PubMed: 20855423]

van't Hof W, Blankenvoorde MF, Veerman EC, Amerongen AV. The salivary lipocalin von Ebner's gland protein is a cysteine proteinase inhibitor. J Biol Chem. 1997; 272:1837–1841. [PubMed: 8999869]

Viswanathan M, Kim SK, Berdichevsky A, Guarente L. A role for SIR-2.1 regulation of ER stress response genes in determining C. elegans life span. Dev Cell. 2005; 9:605–615. [PubMed: 16256736]

Valencia-Sanchez MA, Liu J, Hannon GJ, Parker R. Control of translation and mRNA degradation by miRNAs and siRNAs. Genes Dev. 2006; 20:515–524. [PubMed: 16510870]

Wang S, Kaufman RJ. The impact of the unfolded protein response on human disease. J Cell Biol. 2012; 197:857–867. [PubMed: 22733998]

WHO (World Health Organization). International Programme on Chemical Safety Geneva, 1990. Environmental Health Criteria 101 Methylmercury.

Yee S, Choi BH. Oxidative stress in neurotoxic effects of methylmercury poisoning. Neurotoxicology. 1996; 17:17–26. [PubMed: 8784815]

Yoshida M, Honda M, Watanabe C, Satoh M, Yasutake A. Neurobehavioral changes and alteration of gene expression in the brains of metallothionein-I/II null mice exposed to low levels of mercury vapor during postnatal development. J Toxicol Sci. 2011; 36:539–547. [PubMed: 22008530]

Yoshida H, Matsui T, Yamamoto A, Okada T, Mori K. XBP1 mRNA is induced by ATF6 and spliced by IRE1 in response to ER stress to produce a highly active transcription factor. Cell. 2001; 107:881–891. [PubMed: 11779464]

Highlights

- Chronic Methylmercury exposure increases oxidative stress and endoplasmic reticulum stress gene expression
- Chronic Methylmercury exposure increases lpr and decreases abu family gene expression
- Chronic Methylmercury exposure increases lpr and decreases abu family gene expression

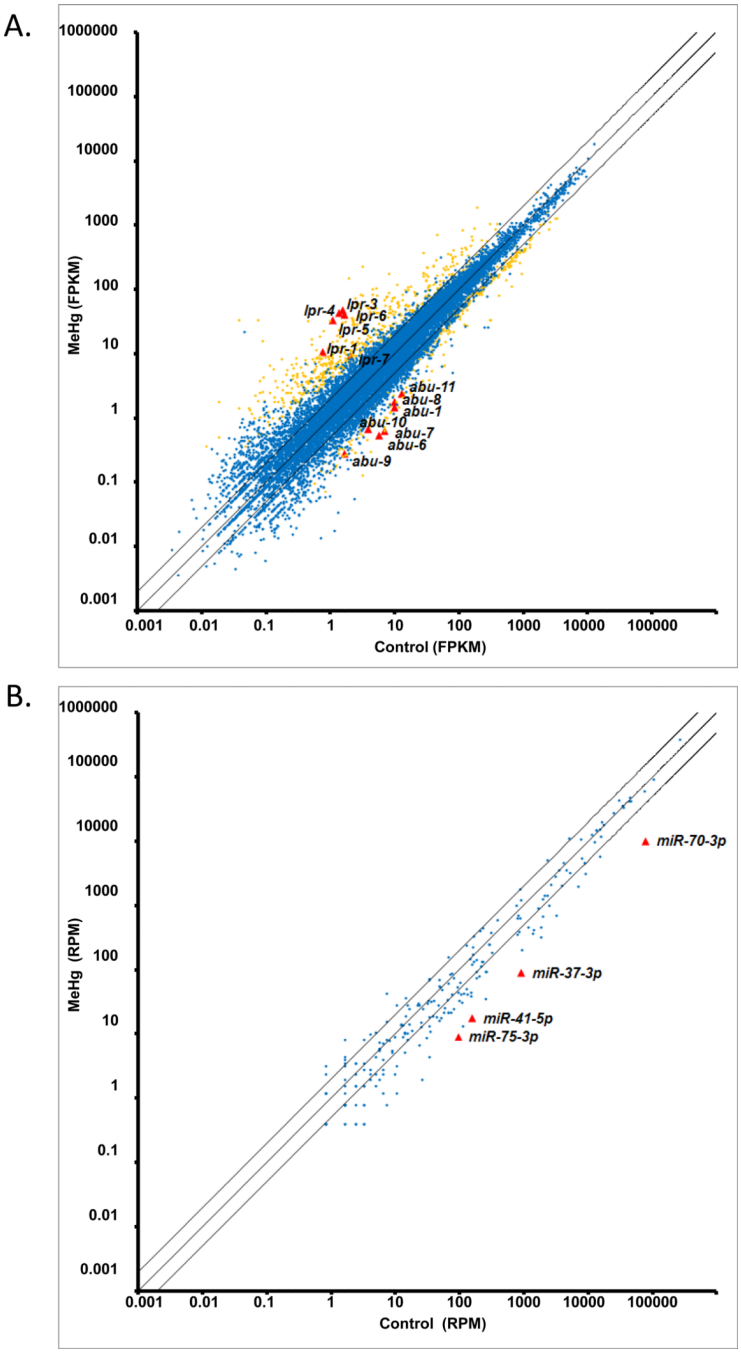

Figure 1.

Scatter plot of RNA-seq (A) and miRNA-seq (B) from control and MeHg (10μM) treated animals. RNAs were isolated from whole animals treated from embryo to L4 stage and libraries prepared and sequenced as described in Methods. Data were plotted as fragments per kilobase of exon per million fragments mapped (FPKM) or reads per million mapped reads (RPM) as indicated. Upper and lower diagonal lines represent 2-fold or 0.5-fold ratio, respectively. Yellow dots (A) represent genes with a false discovery rate corrected significant change ($q < 0.05$) between treatments. The location of *lpr* family, *abu* family genes, and significant miRNAs are indicated with a red triangle.

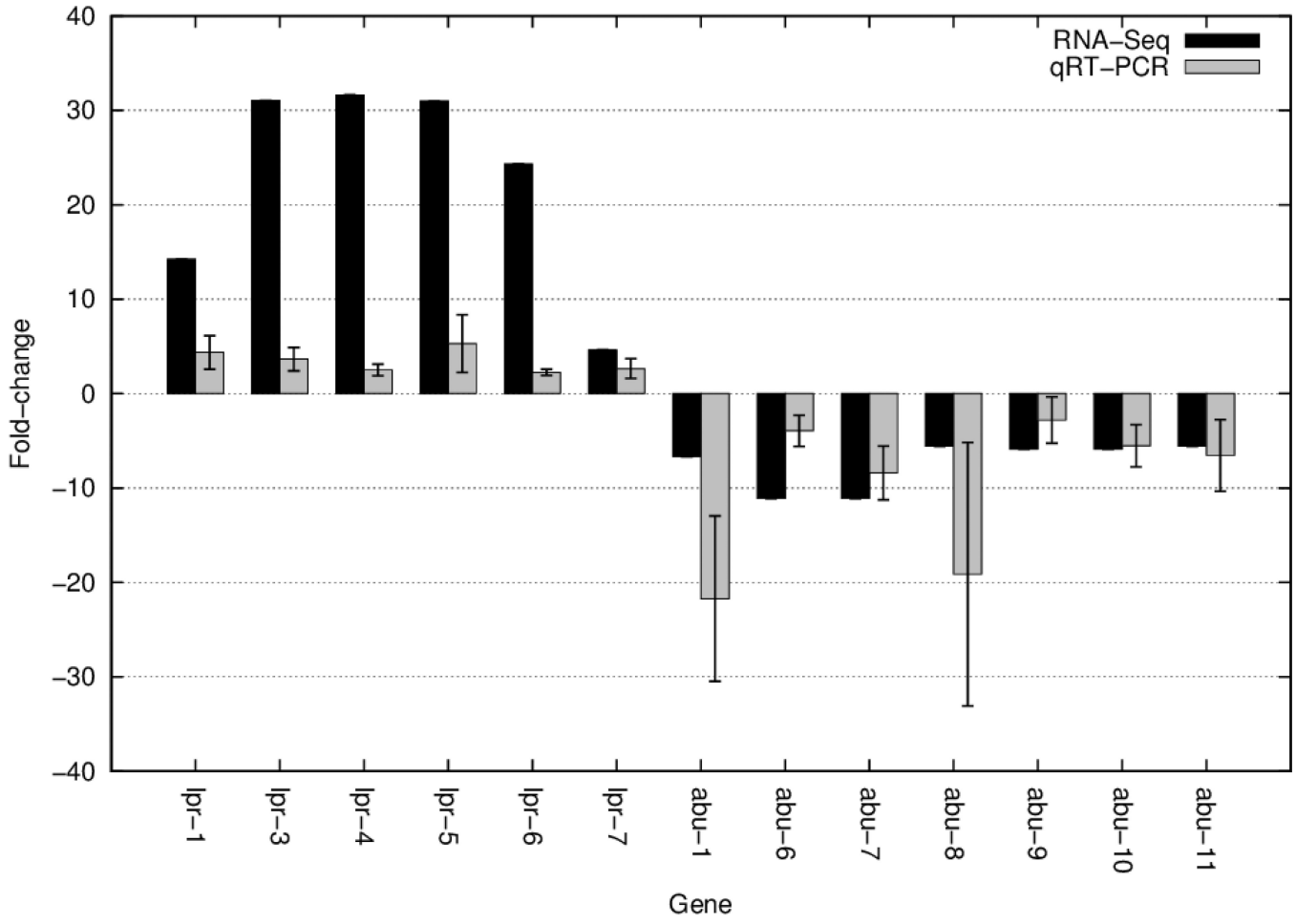

Figure 2.

Gene expression changes in LPR and ABU family genes. RNA-seq and qRT-PCR were performed as described in Methods. Filled black bars represent RNA-seq fold changes for the indicated genes comparing control to MeHg-treated animals (10μM from embryo to L4 stage). Filled grey bars represent qRT-PCR results as the average from 4 independent samples ± SD Positive fold changes were calculated based on treated/control. Negative fold changes were calculated based on −1 control/treated.

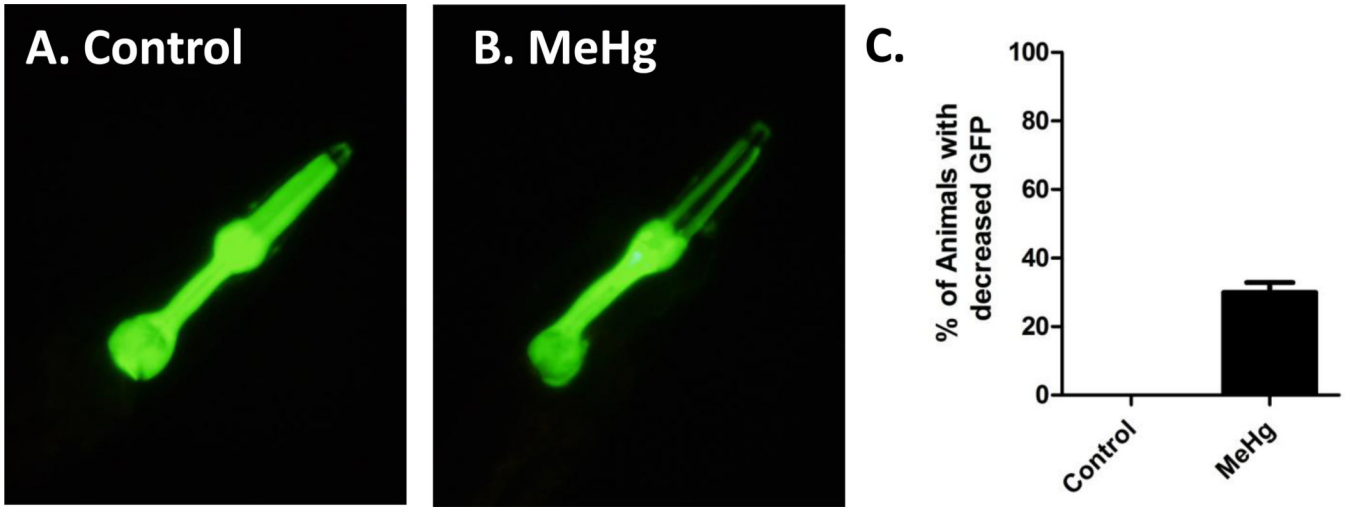

Figure 3.

Fluorescence intensity changes in pharynx of P*abu-1::GFP* strain young adults after exposure to MeHg (125μM). Transgenic integrated animals were grown to L4 stage and treated with the MeHg for 24h. Animals were then placed on an agar pad and micrographs taken of the pharynx of either control (A) or MeHg treated (B) animals. Photo in (B) represents decreased GFP intensity. Plates of animals were also scored for loss of GFP intensity. Values in panel (C) represent mean percent and standard deviation of animals with decreased GFP intensity from 4 independent experiments of 99–159 animals each. Animals were scored as decreased GFP intensity if the procorpus region had consistent and unambiguous decrease of at least 50% in fluorescence. No animals with decreased GFP were observed in control plates.

Toxicol Lett. Author manuscript; available in PMC 2014 October 24.

Table 1

Twenty (20) most up-regulated transcripts and twenty (20) most down-regulated transcripts in MeHg-treated compared to non-treated *C. elegans*. FPKM values are fragments per kilobase of exon per million fragments mapped.

Transcript ID	WormBase locus ID (if available)	FPKM in control	FPKM in MeHg treated	Fold change $FPKM_{MeHg}/FPKM_{control}$	FDR-corrected *p*-value (*q*-value)
C32H11.10	*dod-21*	0.04	34.09	901.96	4.23×10^{-9}
C32H11.9		0.07	33.13	443.14	0.00
F44G3.10		0.09	15.66	174.99	5.22×10^{-5}
B0399.2	*oac-1*	0.02	1.78	94.90	7.30×10^{-4}
C08E3.1		1.94	150.74	77.85	6.80×10^{-7}
Y64H9A.2		0.45	32.52	71.91	0.00
C08E3.13		3.19	226.42	70.89	0.00
K08C7.5	*fmo-2*	0.11	6.67	57.98	1.40×10^{-12}
E03H4.10	*clec-17*	0.09	4.32	46.72	3.96×10^{-7}
F55F8.1	*ptr-10*	0.08	3.79	46.66	4.90×10^{-11}
R03H4.6	*bus-1*	0.18	8.21	46.40	1.85×10^{-13}
T08G5.3		0.13	5.81	44.32	6.62×10^{-5}
Y51B9A.4	*arrd-2*	0.04	1.44	38.31	1.53×10^{-2}
F26D11.2		0.07	2.24	33.52	3.45×10^{-4}
EGAP7.1	*dpy-3*	0.98	32.70	33.36	0.00
R07E3.6		0.51	16.94	33.16	0.00
C08E3.10	*fbxa-158*	0.08	2.52	31.84	2.64×10^{-4}
W04G3.3	*lpr-4*	1.37	43.42	31.65	0.00
W04G3.8	*lpr-3*	1.54	47.76	31.05	0.00
W04G3.2	*lpr-5*	1.07	33.23	30.98	0.00
-	-	-	-	-	-
T06E4.9		9.65	1.18	0.12	3.68×10^{-4}
F59B10.3		3.73	0.45	0.12	1.48×10^{-3}
ZC262.10		2.46	0.29	0.12	3.93×10^{-3}
ZC262.9		2.46	0.29	0.12	3.93×10^{-3}

Transcript ID	WormBase locus ID (if available)	FPKM in control	FPKM in MeHg treated	Fold change $FPKM_{MeHg}/FPKM_{control}$	FDR-corrected *p*-value (*q*-value)
F28F8.2	*acs-2*	18.51	2.17	0.12	9.95×10^{-14}
C05A9.1	*pgp-5*	55.68	6.32	0.11	9.95×10^{-14}
C15A11.6	*col-62*	301.83	33.98	0.11	0.00
Y51H4A.9	*col-137*	34.60	3.89	0.11	3.38×10^{-7}
T21E8.2	*pgp-7*	26.31	2.93	0.11	1.95×10^{-10}
T21E8.1	*pgp-6*	58.97	6.55	0.11	0.00
C15A11.5	*col-7*	312.88	33.27	0.11	0.00
W06G6.10		6.88	0.71	0.10	1.90×10^{-3}
C03A7.4	*pqn-5*	6.96	0.70	0.10	2.23×10^{-5}
C03A7.7	*abu-6*	5.73	0.53	0.09	2.08×10^{-5}
C01G12.11	*nspb-9*	6.94	0.63	0.09	1.06×10^{-2}
C03A7.8	*abu-7*	6.92	0.63	0.09	5.74×10^{-6}
Y37E11B.9		0.83	0.07	0.09	4.22×10^{-2}
T06E4.11	*pqn-63*	4.22	0.30	0.07	6.14×10^{-6}
T06E4.10		3.19	0.13	0.04	1.76×10^{-3}
Y47D7A.9		18.25	0.37	0.02	7.44×10^{-3}

Table 2

Enriched GO Biological Process, Molecular Function and Cellular Comparment terms among differentially expressed genes in response to MeHg treatment. Genes and % correspond to the number and percentage of the regulated genes that have the GO term annotation in question. p-value is a measure of enrichment (Fisher exact test) of the GO term among the genes.

Enriched biological process for up-regulated genes	**Genes**	**%**	**q-value**
collagen and cuticulin-based cuticle development	15	2.9	8.5×10^{-9}
positive regulation of multicellular organism growth	25	4.9	1.7×10^{-7}
protein maturation	7	1.4	1.8×10^{-6}
protein processing	7	1.4	1.8×10^{-6}
oviposition	15	2.9	5.1×10^{-3}
nematode larval development	54	10.6	9.5×10^{-3}
proteolysis	21	4.1	1.2×10^{-2}
post-embryonic body morphogenesis	3	0.6	1.6×10^{-2}
steroid metabolic process	4	0.8	2.7×10^{-2}
Enriched biological process for down-regulated genes			
dephosphorylation	6	2.7	2.7×10^{-3}
vitelline membrane formation	3	1.3	9.0×10^{-3}
protein modification process	12	5.3	1.1×10^{-2}
aminoglycan metabolic process	3	1.3	2.2×10^{-2}
Enriched molecular function for up-regulated genes			
hedgehog receptor activity	8	1.6	4.0×10^{-7}
3-beta-hydroxy-delta5-steroid dehydrogenase activity	3	0.6	1.1×10^{-2}
steroid dehydrogenase activity, acting on the CH-OH group of donors, NAD or NADP as acceptor	3	0.6	1.1×10^{-2}
calcium ion binding	9	1.8	2.2×10^{-2}
serine-type endopeptidase activity	4	0.8	4.4×10^{-2}
Enriched molecular function for down-regulated genes			
phosphatase activity	11	4.9	1.6×10^{-5}
adenyl ribonucleotide binding	17	7.6	4.0×10^{-3}
ATPase activity, coupled to transmembrane movement of substances	5	2.2	4.6×10^{-3}
P-P-bond-hydrolysis-driven transmembrane transporter activity	5	2.2	6.0×10^{-3}
metallopeptidase activity	6	2.7	1.6×10^{-2}
pyrophosphatase activity	9	4.0	2.3×10^{-2}
Enriched cellular component for up-regulated genes			
integral to membrane	190	37.2	1.2×10^{-5}
intrinsic to membrane	190	37.2	1.4×10^{-5}
external side of plasma membrane	3	0.6	3.5×10^{-3}
endoplasmic reticulum	9	1.8	1.6×10^{-2}
Enriched cellular component for down-regulated genes			
cytoskeleton	13	5.8	3.0×10^{-6}
cytoskeletal part	7	3.1	1.4×10^{-3}

Enriched biological process for up-regulated genes	**Genes**	**%**	**q-value**
intracellular non-membrane-bounded organelle	14	6.2	2.2×10^{-3}
intermediate filament	3	1.3	6.0×10^{-3}
intermediate filament cytoskeleton	3	1.3	6.0×10^{-3}
myosin complex	3	1.3	2.3×10^{-2}
actin cytoskeleton	3	1.3	4.9×10^{-2}